Available online at www.sciencedirect.com
SCIENCE DIRECT®
Deep-Sea Research I 52 (2005) 1138–1154
DEEP-SEA RESEARCH PART I
www.elsevier.com/locate/dsr

Dissolved oxygen extrema in the Arctic Ocean halocline from the North Pole to the Lincoln Sea

Kelly Kenison Falkner[a,*], Michael Steele[b], Rebecca A. Woodgate[b], James H. Swift[c], Knut Aagaard[b], James Morison[b]

[a]*College of Oceanic & Atmospheric Sciences, 104 Ocean Admin Bldg., Oregon State University, Corvallis, OR 97331-5503, USA*
[b]*Applied Physics Laboratory, University of Washington, 1013 NE 40th Street, Seattle, WA 98105-6698, USA*
[c]*UCSD Scripps Institution of Oceanography, 9500 Gilman Dr., La Jolla, CA 92093-0214, USA*

Received 17 May 2004; received in revised form 24 November 2004; accepted 21 January 2005
Available online 26 April 2005

Abstract

Dissolved oxygen (O_2) profiling by new generation sensors was conducted in the Arctic Ocean via aircraft during May 2003 as part of the North Pole Environmental Observatory (NPEO) and Freshwater Switchyard (SWYD) projects. At stations extending from the North Pole to the shelf off Ellesmere Island, such profiles display what appear to be various O_2 maxima (with concentrations 70% of saturation or less) over depths of 70–110 m in the halocline, corresponding to salinity and temperature ranges of 33.3–33.9 and −1.7 to −1.5 °C. The features appear to be widely distributed: Similar features based on bottle data were recently reported for a subset of the 1997–1998 SHEBA stations in the southern Canada Basin and in recent Beaufort Sea sensor profiles. Oxygen sensor data from August 2002 Chukchi Borderlands (CBL) and 1994 Arctic Ocean Section (AOS) projects suggest that such features arise from interleaving of shelf-derived, O_2-depleted waters. This generates *apparent* oxygen maxima in Arctic Basin profiles that would otherwise trend more smoothly from near-saturation at the surface to lower concentrations at depth. For example, in the Eurasian Basin, relatively low O_2 concentrations are observed at salinities of about 34.2 and 34.7. The less saline variant is identified as part of the lower halocline, a layer originally identified by a Eurasian Basin minimum in "NO," which, in the Canadian Basin, is reinforced by additional inputs. The more saline and thus denser variant appears to arise from transformations of Atlantic source waters over the Barents and/or Kara shelves. Additional low-oxygen waters are generated in the vicinity of the Chukchi Borderlands, from Pacific shelf water outflows that interleave with Eurasian waters that flow over the Lomonosov Ridge into the Makarov Basin and then into the Canada Basin. One such input is associated with the well-known silicate maximum that historically has been associated with a salinity of ≈ 33.1. Above that ($32 < S < 33$), there is a layer moderately elevated in temperature (summer Bering Sea water) that we show is also O_2-depleted. We propose that these low O_2 waters influence the NPEO and SWYD profiles to varying extents in a manner reflective of the large-scale circulation. The patterns of halocline circulation we infer from the intrusive features defy a simple boundary-following cyclonic flow. These results demonstrate the value of the improved

*Corresponding author. Institute of Limnology, Austrian Academy of Sciences, Mondeestr. 9, Mondsee 5310, Austria. Tel.: +541 737 3625; fax: +541 737 2064.
E-mail address: kfalkner@coas.oregonstate.edu (K.K. Falkner).

0967-0637/$ - see front matter
doi:10.1016/j.dsr.2005.01.007

resolution made feasible with continuous O_2 profiling. In the drive to better understand variability and change in the Arctic Ocean, deployment of appropriately calibrated CTD-O_2 packages offers the promise of important new insights into circulation and ecosystem function.

Keywords: Polar oceanography; Dissolved oxygen; Chemical sensor; Halocline

1. Introduction

Beginning in 2002, reliable new-generation dissolved O_2-sensors have been deployed in the Arctic Ocean from aircraft, ships and on buoys. While the Arctic environment continues to pose challenges for attaining optimal data quality from sensors, these are providing detailed information regarding O_2 distributions. Such profiles reveal halocline oxygen extrema at locations extending from the North Pole to the Lincoln Sea (Fig. 1a). To develop an understanding of the origin of the halocline features, we turn upstream and examine recent ship-based O_2-sensor data from the Chukchi Borderlands in 2002 as well as some earlier generation sensor data from the 1994 Arctic Ocean Section.

2. Background

It has long been known that deviations from O_2-saturation in surface waters of marginal seas of the Arctic can be considerable by world ocean standards. Levels of supersaturation (160%), among the highest anywhere, have been reported for ice-free waters of the East Siberian and Chukchi seas in the summer under bursts of extremely high productivity (Codispoti and Richards, 1971). Respiratory activities and winter cooling can reduce concentrations to around 90% of saturation under the ice cover in the southernmost Canada Basin (Sherr and Sherr, 2003) and elsewhere along the margins. What is less well appreciated is that nearly all available data show the central Arctic surface mixed layer O_2 concentrations to be near equilibrium with respect to exchange with the atmosphere (360–420 mmol m^{-3}). Despite having a year-round ice cover, the central Arctic surface O_2 concentrations are within 2–3% of saturation as is true for much of the world's oceans. While this could result from a fortuitous balance of biological production and respiration, it seems more likely that the ice cover is permeable to gas exchange on the timescale of circulation of surface waters within the Arctic interior. Basin-wide satellite monitoring over the last few decades has revealed a very dynamic ice cover with significant fraction of leads even in winter and so perhaps near gas exchange equilibrium should not be surprising.

Typically, O_2 concentrations below the mixed layer decline with depth due to isolation from the atmosphere and consumption due to respiratory activities. Because Arctic halocline waters do not form only by vertical mixing of surface waters with those at depth (Aagaard et al., 1981 and others), the shapes of O_2 profiles reflect the advective imprint of waters from various regions. In the following discussion, we focus on the halocline

Fig. 1. (a) Bathymetric map of the North Pole to Lincoln Sea sector of the Arctic Ocean. Numbered red dots are locations of NPEO'03 station locations. Numbered orange dots are the SWYD'03 station locations. (b) Bathymetric map of the Arctic Ocean. The general sense of the average large-scale surface circulation is indicated by the broad shaded arrows. Note that the relative widths and positioning of the Transpolar Drift and the Beaufort Gyre are variable and thought to be a function of atmospheric circulation patterns. The subsurface cyclonically steered flow of Atlantic water is illustrated by the red arrows, with the dashed portions being highly uncertain. Pacific waters circulate largely within the halocline and its inflows and outflows are indicated by the blue arrows. Red and orange station markers are as shown in Fig. 1a. Yellow diamond is NPEO'02-S3 location. CBL station locations are shown in dark red symbols: star = S21, circle = S14, square = S123, downward pointing triangle = S85, upward pointing triangle = S110. AOS94 station locations are shown by the black stars and correspond from left to right to the following stations: 9, 13, 17, 18, 26, 33, 36. Also indicated are the locations of historical data sets (AIWEX, Station A, T3, CESAR) discussed in the text.

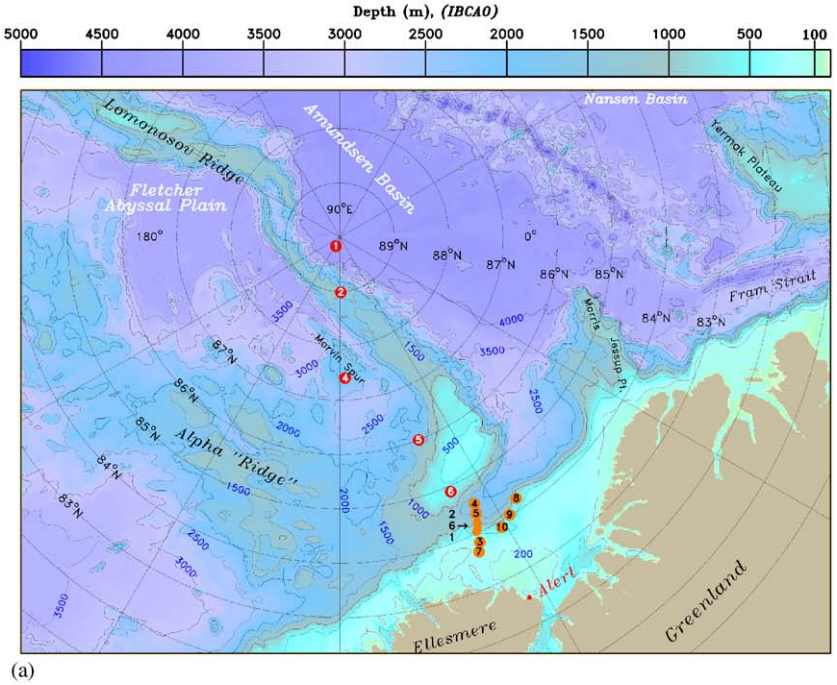
Depth (m), (IBCAO)
5000 4500 4000 3500 3000 2500 2000 1500 1000 500 100
Lomonosov Ridge
Amundsen Basin
Nansen Basin
Yermak Plateau
Fletcher Abyssal Plain
Fram Strait
Morris Jassup Pt.
Marvin Spur
Alpha "Ridge"
Alert
Ellesmere
Greenland

(a)

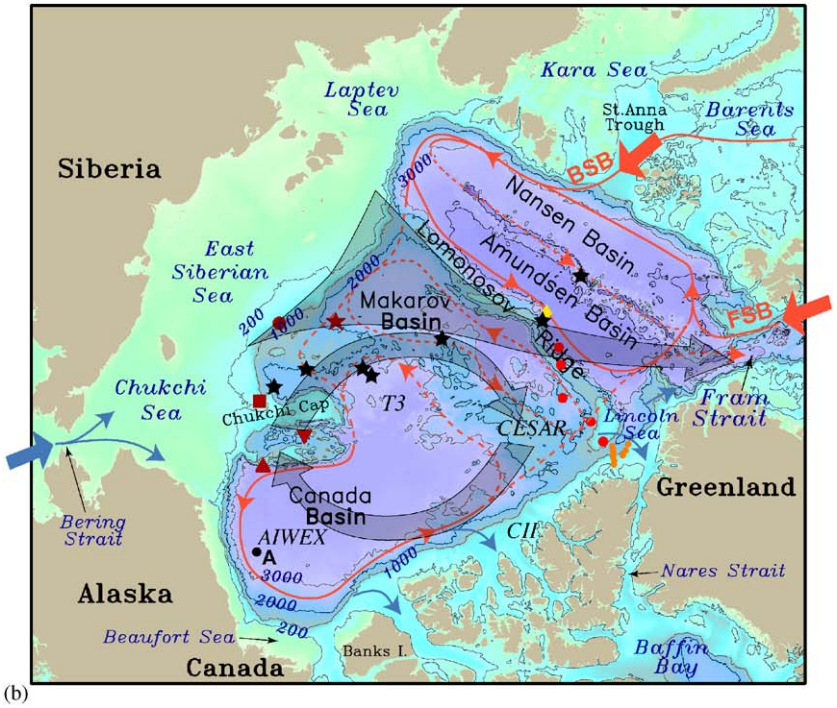
Kara Sea
Laptev Sea
St.Anna Trough
Barents Sea
Siberia
BSB
Nansen Basin
Amundsen Basin
Lomonosov Ridge
East Siberian Sea
Makarov Basin
FSB
Chukchi Sea
Chukchi Cap
T3
CESAR
Lincoln Sea
Fram Strait
Greenland
Canada Basin
Bering Strait
AIWEX
A
CII
Nares Strait
Alaska
Beaufort Sea
Banks I.
Baffin Bay
Canada

(b)

layers, i.e., waters lying beneath the upper mixed layer and above the relatively warm ($T \geqslant 0\,^{\circ}C$; $\approx 200-600\,m$) core of the Atlantic layer. We begin in the Nansen Basin where Atlantic waters clearly dominate and make our way around to the Canadian Basin where river water and Pacific inputs come into play. It should be noted that a number of changes in the disposition and properties of various water types in the Arctic Ocean have been reported over the past decade or so. Below we concern ourselves with persistent water type distinctions and changes pertinent to the halocline layers of interest.

Downstream of the Kara Sea, two main branches of Atlantic water are found, one originating at Fram Strait (FSB) and the other from the Barents and Kara Seas (BSB) (Fig. 1b). We note that the BSB is relatively cooler, fresher, and better ventilated than is the FSB (McLaughlin et al., 2002; Schauer et al., 2002), but their property differences are relatively small compared to the range in properties throughout the halocline. As a whole, the Atlantic layer remains relatively well ventilated (about 290–320 $mmol\,m^{-3}$ O_2) throughout most of the Arctic Basin. Somewhat higher O_2 concentrations are typically found in the topographically steered cyclonic boundary currents than in adjacent basin interiors, where circulation is thought to be more sluggish. Similarly to temperature and salinity, O_2 decreases within the warm core along the advective pathways of the boundary current in the Makarov and Canada basins (Swift et al., 1997). Highest values ($320\,mmol\,m^{-3}$) are found near the confluence of the BSB and FSB in the Nansen Basin near the St. Anna Trough. Lowest values ($\approx 290\,mmol\,m^{-3}$) have been reported for the warm core of the Atlantic water in the Beaufort Sea and these vary in time by a few percent in a manner that may result from upstream changes in the relative amounts and properties of the two branches of Atlantic water (McLaughlin et al., 2002).

Just above the warm Atlantic water core, beginning near the confluence of its source branches, oxygen is somewhat depleted and a local minimum occurs ($\leqslant 310\,mmol\,m^{-3}$) that is centered at a salinity of about 34.7 (e.g. see Wilson and Wallace, 1990 and data from ARX87, ARX96, AOS94, and herein). This lies deeper than the O_2 minimum of the Lower Halocline Water (LHW) discussed below. The origins of this deeper layer will be more fully discussed in a future publication but presumably its circulation is similar to that of the Atlantic layer core, since its O_2 concentrations decrease along the advective pathway of the boundary current, reaching a low of $\approx 290\,mmol\,m^{-3}$ at Station A (Fig. 1b) in the Beaufort Sea (McLaughlin et al., 2002). The magnitude of depletion is marginally greater than for the warm core, implicating lateral injection of O_2-depleted waters in this layer as it circulates. We shall show below that this indeed occurs in the Canada Basin.

Local O_2 maxima ($\leqslant 310\,mmol\,m^{-3}$) centered on a salinity of 34.5 were reported for bottle-based profiles over the Alpha Ridge during the T3 ice island occupations (1958, 1969–1971) (Wilson and Wallace, 1990). This structure was most pronounced on the eastern side of the ridge. It was not evident at T3 stations in the Makarov Basin (1968–1969), nor in the Beaufort Sea at the Arctic Internal Wave Experiment (AIWEX) site (74°N 144°W; 1985), nor at the Canadian Ice Island (CII) site (80°57′N 97°36′W; 1985) (Fig 1b). At each of these sites, vertical resolution of the bottle sampling appears to have been sufficient to capture such a feature should it have existed. The situation for the Canadian Expedition to Study the Alpha Ridge (CESAR; 85°45′N 111°W; 1983) is less clear. One depiction of these data shows what appears to be a one-point maximum at $S \approx 34.1$ (Fig. 4d in Jones and Anderson, 1986), but this point appears to have been eliminated in a subsequent publication (Fig. 2 in Wallace et al., 1987). It was proposed that where the local O_2 maximum did occur, it circulated with an overlying layer known in the literature as LHW (Wilson and Wallace, 1990).

LHW ($34.2 < S < 34.3$) occurs just above the Atlantic layer and was originally identified by a weak minimum in the quasi-conservative NO parameter ($NO = [O_2] + 9 \times [NO_3]$; Broecker, 1974) thought to have been established during dense water formation over the BSB shelves (Jones and Anderson, 1986). Oxygen concentrations in this layer show a deficit relative to waters above

and below of about 10 mmol m^{-3}. This feature is in fact hard to recognize in a vertical O_2 profile having typical bottle spacing that exceeds 20 m. Based on archived (1963–1972) data for Arctic shelf seas, it was subsequently shown that low NO is not unique to the Barents and Kara shelves (Wilson and Wallace, 1990). Based on available data, it was proposed instead that NO/PO ($PO = [O_2] + 135 \times [PO_4]$; Broecker, 1974) provides more unique geographic specificity. By the NO/PO criterion, inputs to LHW from the Laptev Sea were implicated in maintenance of the oxygen minimum (Wilson and Wallace, 1990).

Rudels et al. (1996) argued that LHW achieves low NO in the Barents Sea and adjoining Nansen Basin over several seasons (Rudels et al., 1996) via (1) stripping of shelf-derived nutrients by biological productivity in surface waters, (2) loss of O_2 produced during photosynthesis by exchange with the atmosphere, and (3) winter convection driving the surface NO signature to the depth of the lower halocline. Away from its formation sites, fresh waters from the large Eurasian rivers and seasonal sea ice melt cap the LHW and serve to inhibit further convective renewal.

In the absence of further inputs, the NO value should remain approximately constant since respiratory biological activity is taken into account in its formulation. However, available data suggest that additional lateral contributions to LHW occur on the Canadian Basin side of the Lomonosov Ridge. Higher temperatures and silicate concentrations than in the Eurasian sector accompany the NO minimum in portions of the Canadian Basin (Salmon and McRoy, 1994). Moreover, significantly lower NO minima have been reported for the Canadian Basin than for the Eurasian Basin (Guay and Falkner, 1997; McLaughlin et al., 1996). The NO minimum in the Canada Basin correlates inversely with Ba concentration (Guay and Falkner, 1997), and high-Ba concentrations at this depth originate from the Bering Strait inflow. Denitrification (lowering both O_2 and NO_3) believed to be occurring in association with biological activity over the highly productive Chukchi and east Siberian shelf regions (Codispoti et al., 1991), combined with Ba recycling, are thought to account for alteration of LHW properties (Guay and Falkner, 1997).

Above LHW, there is a persistent well-known nutrient maximum and O_2 minimum layer that historically has been centered at a salinity of about 33.1, but has shifted in at least some regions to somewhat lower salinities (32.9) in the 1990s (McLaughlin et al., 2002). The feature is most readily recognized and traced by high silicate concentrations (Jones and Anderson, 1986; Jones et al., 1991; Kinney et al., 1970). This water type was observed in both the Makarov and Canada Basins prior to about 1993 when it was no longer seen in most of the Makarov Basin (McLaughlin et al., 1996). We refer to it as winter Bering Sea Water (wBSW). Its properties are close to, but do not exactly match, waters passing through Bering Strait during times of low primary productivity (Coachman and Barnes, 1961; Cooper et al., 1997). Some interaction with shelf sediments and dense water formation is required to explain the full suite of chemical and physical properties of wBSW (Cooper et al., 1997; Moore and Smith, 1986). The layer tends to be relatively cold, though it is above freezing. Near the shelf, O_2 concentrations in this water can be as low as 130 mmol m^{-3} (Swift et al., 1997). Seaward of the slope in the Beaufort Sea, the O_2 concentration in the 32.9–33.3 salinity range is about 270 mmol m^{-3} (McLaughlin et al., 2002; Swift et al., 1997). Intermittent contributions of dense water produced by ice formation over adjacent shelves help support low temperatures in this layer, but nutrient concentrations suggest these contributions are relatively minor (Melling and Moore, 1995).

Shallower still, elevated temperatures (typically $-1.5 < T < -0.5$) distinguish two other varieties of Bering Sea water within the Arctic Ocean. Following recent designations (Steele et al., 2004), we refer to the saltier variant ($32 < S < 33$) as summer Bering Sea Water (sBSW). It is most prevalent in the northern portion of the Beaufort Gyre and arises from mixing of Bering Shelf and Gulf of Anadyr waters (Coachman et al., 1975), spreading northward through Herald Canyon and the Central Valley. The other variant is Alaskan Coastal Water (ACW) ($31 < S < 32$), which is most clearly identified in the southern Beaufort Sea.

While our understanding of the chemical properties, circulation pathways, and variability over the shelves of these different waters is still evolving (Weingartner et al., 1998), to a first approximation, the influence of these Bering Sea waters within the Arctic Basin may depend on larger scale atmospheric pressure patterns (Steele et al., 2004). Since our Alert to North Pole data do not show a distinctive O_2 signal in ACW, we do not discuss it or shallower layers further.

Recently, McLaughlin et al. (2004) reported the occurrence of local O_2 maxima in the halocline for several bottle casts collected over the Chukchi Plateau and Mendeleev Abyssal Plain as part of the SHEBA drift program in 1997–1998. Peak values were about 340 mmol m^{-3} at 120–140 m for $33.8 < S < 34.0$. These maxima were associated with relatively low nutrients and with temperatures a few tenths of a degree above freezing. Just above the maxima at $33.0 < S < 33.2$ were local O_2 minima associated with higher nutrients and somewhat warmer water temperatures. It was noted that tightly spaced bottle profiles collected in 1969 north of the SHEBA stations at ice station T3 over the Mendeleev Abyssal Plain (Kinney et al., 1970) did not display such local O_2 maxima. McLaughlin et al. (2003) proposed that the O_2 maxima heralded a change in the supply of LHWs to the Canada Basin. Based on the geographic distribution and chemical properties, and concordant with a 1990 Atlantic-Pacific water mass boundary shift from the Lomonsov to Mendeleev Ridge (McLaughlin et al., 1996), they proposed that such maxima arise from convection due to ice formation in nutrient-depleted shelf waters of the East Siberian Sea. We are also aware of recently collected oxygen profiles data in the Beaufort Sea that show similar O_2 maxima (peak concentrations of 70% saturation in 2001) centered on a salinity of about 33.8 (Shimada et al., 2005). It has been hypothesized these features might originate from convection in polynyas known to be occurring in the southern Beaufort Sea.

3. Sampling and analytical methods

Oceanographic profile data were collected via aircraft from the Arctic Ocean in 2003 as part of the North Pole Environmental Observatory (NPEO) and Freshwater Switchyard (SWYD) programs (Fig. 1a). Details regarding methodology and analytical processing can be found along with the archived data at the National Snow and Ice Data Center (Falkner, 2000–2001, 2002, 2003; Morison et al., 2002). Briefly, for NPEO a fixed-wing plane (de Havilland DHC-6 Twin Otter) landed at each station on the ice. Casts were conducted on a Kevlar cable using a generator-driven winch from within a nylon shelter attached to the aircraft cargo doors. A Seabird SBE19 CTD carrying a SBE43 dissolved O_2 sensor (CTD-O_2) was mounted above a weight near the bottom of the cable. Four Niskin bottles, customized for through-ice work (General Oceanics model 1010 with 8″ extension and modified plunger) were hung above at increments and tripped via messengers. The package was raised and lowered at 40–50 m/min.

Immediately upon their retrieval into the warmed aircraft, the Niskin bottles were sampled for dissolved O_2, followed by salinity and other parameters. Dissolved O_2 samples were drawn directly into calibrated 150-ml glass flasks and preserved upon collection, according to standard procedures (Dickson, 1994). Samples were analyzed by Winkler titration at the Alert base station within 24 h of sample collection. For this, the contents of the flasks were allowed to come to room temperature, initially rapidly titrated to avoid loss of iodine, and then titrated in a light box to a starch indicator (visual) endpoint. Precision based on separately drawn replicates is estimated to be about 1%. Problems described in detail in the archived metadata limited the number of trustworthy (accurate) bottle O_2 analyses for the five profiles.

Salinity samples were collected into 125-ml glass bottles, the caps of which were fitted with conical polyethylene inserts. The samples were prevented from freezing at any time. Caps were wrapped in Parafilm. Salinities were analyzed within 2 weeks of their collection at Oregon State University, using a Guildline Autosal standardized with IAPSO standard seawater. Precision based on separately drawn replicates for these determinations was 0.002 psu. Niskin bottle closure depths

from the meter wheel were refined by matching bottle salinities to profile salinities. Similar procedures were used during the NPEO 2002 operation, except that bottle O_2 sampling was not successful.

Switchyard 2003 sampling was conducted via helicopter (Bell 206 Long Ranger) through leads in the ice. A portable winch and gantry were used to deploy a SBE19+ CTD instrument outfitted with an SBE43 dissolved O_2 sensor. The package was lowered at about 30 m/min. Near-surface water samples were obtained separately deploying a 5-l Niskin bottle. It was not feasible to sample for O_2 in the field during SWYD 2003. There was no shelter and so to avoid rapid seawater freezing, the contents of the Niskin were quickly transferred to $1-L$ high-density polyethylene bottles and kept from freezing until arrival at the Alert base station. Water was then sub-sampled into separate aliquots for salinity and other parameters as described for the NPEO program.

The Seabird SBE43 has a response lag of order 7 s at our operating temperatures, and so responded less rapidly than did the other CTD sensors. The sensor exhibits less pressure hysteresis above 1000 m than did previous generation sensors, and that which does remain was most apparent across steep gradients of temperature and salinity. We followed the Seabird recommended correction procedure of determining a response lag factor by minimizing differences between up and down casts for the O_2-temperature relationship. The largest deviations between the up and downcasts that remained after this lag correction (7 s), were generally less than 0.5% for the SWYD sensor and less than 1% for the NPEO sensor. Because the instrument package induces a wake and the pump intake was oriented downward, we report downcast data when possible.

Oxygen voltages were processed using an algorithm modeled after that of Owens and Millard (1985) and relying upon calibration parameters (Owens and Millard, 1985; Seabird Application Note No. 64). Both the NPEO and SWYD sensors showed data artifacts resulting from membrane stretching caused by freezing of fluid in a pressure compensation bladder. The fluid was distilled water in the case of NPEO and seawater in the case of SWYD. The deformation was most pronounced for the NPEO sensor. This stretching invalidated the pre-deployment calibration and reduced the sensor response. Unfortunately, a post-mission calibration was not made before the membrane was replaced. We adjusted the calibration to compensate for the membrane change during the mission as follows. The sensitivity calibration coefficient was varied for the North Pole station (NPEO'03-S1) until calculated values corresponded to saturation in the surface mixed layer. Other calibration coefficients (voltage offset, residual temperature, and pressure terms) were assumed to be unchanged from the pre-mission calibration because they should not be affected by stretching of the membrane. After this surface correction, the sensor O_2 concentration matched ($\pm 4\,\mathrm{mmol\,m^{-3}}$) a bottle O_2 measurement from 300 m and deeper (to 800 m) concentrations are similarly close to those from recent bottle casts taken near the North Pole from ships (e.g., Swift et al., 1997).

When the NPEO'03-S1 calibration was applied to the NPEO'03-S2 oxygen profile, it also generated saturation concentrations in the surface mixed layer and concurrence ($\pm 4\,\mathrm{mmol\,m^{-3}}$) with a ≈ 300 m bottle O_2 determination. For the NPEO'03-S6 profile, the revised calibration generated saturation concentrations in the surface mixed layer and otherwise produced a profile similar to the nearby SWYD'03-S4. Salinity at NPEO'03-S4 exhibited a two-layer surface structure. The revised calibration generated upper layer O_2 concentrations corresponding to 11% undersaturation. At the base of what appeared to be an underlying remnant mixed layer, O_2 concentrations did reach saturation values before declining with depth. At NPEO'03-S5, the revised calibration generated values at saturation in the surface mixed layer. During our profile one year earlier at NPEO'02-S3, the SBE43 sensor suffered from similar membrane stretching. The calibration was adjusted analogously to the NPEO'03 data to provide concentrations corresponding to saturation in the surface mixed layer.

During SWYD, calculated surface mixed layer oxygen concentrations based on the pre-mission calibration were within 3% of saturation, but displayed a small temporal drift that resulted from

membrane stretching similar to that which affected the NPEO sensor but less pronounced. Unfortunately, a post-mission calibration was not made before the membrane was replaced. The profiles were therefore fit to 100% saturation at 20 m for each of the stations by minor adjustment of the sensitivity calibration coefficient. We note that there was an extensive network of leads in the SWYD region at the time of sampling. This would help promote equilibration of the surface layer with the atmosphere.

Based on comparisons of concentrations at about 500 m for NPEO'03-S1 with recent ship-based bottle data, we estimate that concentrations for NPEO'02, NPEO'03, and SWYD'03 are reliable to $\pm 4\,\mathrm{mmol\,m^{-3}}$. We hope that additional precautions to avoid freezing in the pressure compensation bladder and increased bottle-based values for correction will diminish electronic O_2 concentration errors during future deployments planned for these and similar programs.

We also present oxygen probe data from the USCGC Polar Star 2002 Chukchi Borderlands expedition, collected using an SBE43 oxygen sensor. Reference-quality bottle dissolved oxygen determinations (carried out to WOCE Hydrographic Program (WHP) standards, e.g. Joyce and Corry, 1994) were available at up to 36 levels per profile. The basic corrections, following techniques in standard use during the WHP, emphasizing the surface layer and the deeper layers, were straightforward to carry out. For salinities greater than 34.8, i.e., below about 300 m, down-cast processed CTD oxygen values typically matched up-cast bottle oxygen values at the same salinity within about $0.1\,\mathrm{mmol\,m^{-3}}$. For salinities less than 34, i.e., in the upper 200 m, there was greater vertical variation in concentration, and sensor-bottle differences were somewhat larger, typically about $4\,\mathrm{mmol\,m^{-3}}$ but in a few cases near $27\,\mathrm{mmol\,m^{-3}}$. We note that in every instance, features we illustrate with the 2002 CBL oxygen probe profiles were verified by the closely spaced bottle oxygen samples.

Finally, we present some previously unpublished CCGS *Louis S. St-Laurent* CTD oxygen probe data from the AOS94 trans-Arctic section. These were collected during the principal CTD/hydrographic profiles, with previous-generation "Beckman" oxygen sensors, as part of an unfunded experiment led by one of the authors (JHS). Due to slow sensor response in cold water, poor sensor recovery from chilling, and damage from occasional freezing conditions (sensors were replaced after damage was noted), more than 40 attempts to collect usable dissolved oxygen profiles resulted in only 8 profiles judged suitable for processing. Reference-quality bottle dissolved oxygen determinations (carried out to WHP standards, e.g. Joyce and Corry, 1994) were available at up to 36 levels per profile. Thus the basic corrections, following techniques in standard use during the WHP, and here emphasizing the deeper layers, were straightforward to carry out for the 8 profiles. (Two were from one station; hence seven profiles are presented here.) Below 200 m down-cast processed CTD oxygen values typically matched up-cast bottle oxygen values at the same pressure within about $0.1\,\mathrm{mmol\,m^{-3}}$. (We also note that the processed AOS94 oxygen probe profile data were not passed through a gradient filter. The small-scale noise which remains is insignificant in the context of our analyses.) But in the upper 200 m, where there was greater vertical variation in concentration, CTDO-bottle differences were typically much larger, often $22–45\,\mathrm{mmol\,m^{-3}}$, despite in most cases the surface layer CTDO-bottle difference having been corrected during processing. These large differences arise chiefly from the very long cold-water time constant of the older Beckman-type sensors. We note that in every case the overall *shapes* of the CTD probe profiles closely matched those of the bottle sample profiles. Therefore we discuss only the principal features of the AOS94 oxygen sensor profiles. In every instance, features we illustrate in the AOS94 oxygen probe profiles were verified by the closely spaced bottle oxygen samples.

4. Observations

Vertical profiles of O_2 concentration for NPEO'03 stations and a representative subset of the SWYD'03 stations are shown in Fig. 2. These

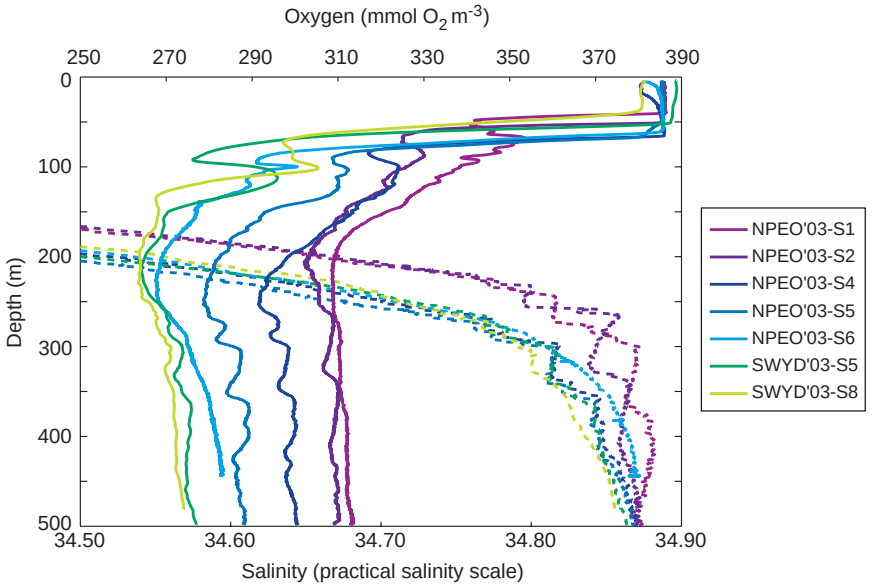

Fig. 2. Salinity and oxygen profiles at locations from the North Pole to the Lincoln Sea that were occupied in May, 2003. For station locations see Fig. 1a. Note that the salinity scale is expanded to best illustrate the intrusive features in the Atlantic layer. See text.

profiles share several characteristics. Just below the mixed layer, in which levels are generally near saturation ($\approx$385 mmol m^{-3}), O_2 concentrations trend sharply lower and subsequently fall off more gradually with increasing depth to ca. 270–310 mmol m^{-3} at about 200 m depth. Superimposed on this overall decrease with depth are several relative O_2 minima (280–340 mmol m^{-3} at ca. 55–95 m), underlain by relative maxima (295–350 mmol m^{-3}; 70–110 m). There are also broader O_2 minima in the 200–250 m depth range. Most of the profiles have a prominent temperature maximum (not shown) just below the mixed layer at 70–90 m depth, characteristic of the ACW contribution, but O_2 decreases smoothly through the depth interval of this temperature signal.

Oxygen concentrations below the mixed layer are highest at the North Pole and diminish southwards toward Ellesmere Island. Below about 250 m, a number of smaller scale (20–40 m) intrusive features occur that are visible across all stations except perhaps NPEO-03 stations 1 and 6. Temperature and salinity profiles show intrusions of similar vertical extent. Similar features in the Atlantic layer have been previously reported by others (e.g., Carmack et al., 1997; Carmack et al., 1998; Quadfasel et al., 1993). Such features arise from interleaving of similarly dense water masses by not purely along-isopycnal mechanism(s) (Carmack et al., 1998). Within the intrusions we observed, O_2 concentration correlates positively with temperature and salinity. This is opposite of what would be expected from interleaving of FSB and BSB waters, since the latter are relatively cold, fresh, and O_2-rich (McLaughlin et al., 2002; Schauer et al., 2002), but is consonant, for example, with leakage across the Lomonosov Ridge of more recently ventilated warm and salty Atlantic waters and subsequent interleaving with older waters. We note that apparent vertical structure differences on scales smaller than 20 m between temperature/salinity and dissolved O_2 in our data are an artifact arising from the relatively slow response of the O_2 sensor. Thus, we restrict our discussion to features with vertical scales larger than 20 m.

Relationships of O_2 with salinity for these stations are depicted in Fig. 3. For added perspective, we have included a representative station from NPEO'02 that, like NPEO'03-S1, is

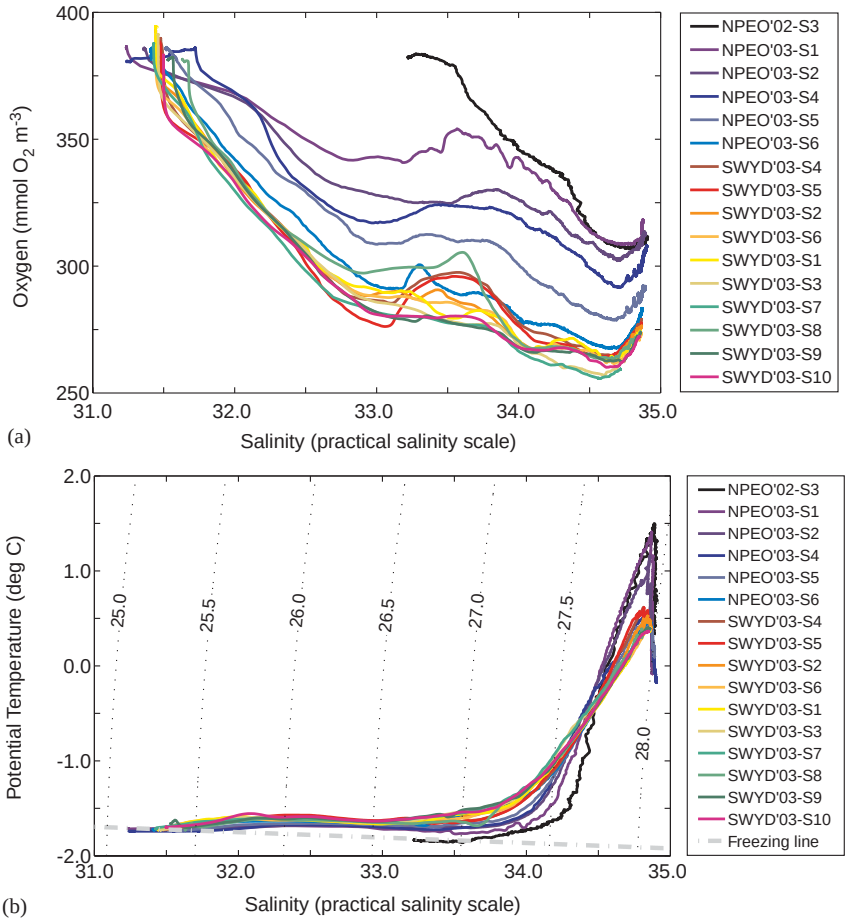

Fig. 3. Upper Panel: Dissolved oxygen vs. salinity at locations from the North Pole to the Lincoln Sea that were occupied in May, 2003. One station from 2002 is also shown. For station locations see Fig. 1a. Lower Panel: Potential temperature vs. salinity for the same stations. Constant density lines (sigma–theta units) are superimposed.

situated near the Amundsen Basin flank of the Lomonosov Ridge (Fig. 1). Its properties differed considerably from those of NPEO'03 and SWYD'03 stations: its upper layers were considerably colder, saltier, and better ventilated (Fig. 3), and there were no O_2 extrema throughout the halocline. Clearly the riverine influence is lacking at NPEO'02. Whether this represents predominantly spatial or temporal variability cannot be addressed by available data. Agreement between NPEO'02-03 and NPEO'03-S1 profiles does improve with increasing depth. Properties converge for $S > 34.5$ as might be expected for stations sharing a common deeper circulation, with NPEO'02-S3 being upstream of NPEO'03-S1 (Schauer et al., 2002).

In contrast, NPEO'03-S1 at the North Pole shares a similar salinity range from the surface to the warm core of the Atlantic layer with other NPEO'03 and SWYD'03 stations (Fig. 3). The halocline becomes warmer and the Atlantic layer becomes cooler progressing from the North Pole toward the Ellesmere shelf. As noted for the depth profiles, these TS changes are generally accompanied by progressively lower O_2 concentrations beneath the mixed layer moving from the North Pole toward the shelf off Ellesmere Island (Fig. 3). Immediately underneath the mixed layer, O_2

concentrations decrease fairly smoothly with increasing salinity, with the O_2-salinity slope of the correlation being more pronounced toward the south.

The smooth decreasing trend in O_2 under the mixed layer is interrupted by variable structure over the salinity range $32.8 < S < 34.7$ (Fig. 3). For example, at NPEO'03-S2 and S4 and SWYD'03-S4 and S5 there are single broad O_2 peaks in this salinity range whereas at the other stations there is more than more than one peak. At NPEO'03-S1 at the North Pole there is evidence for intrusive layering within the main peak. We note especially that the O_2 peaks in the salinity range 32.8–34.7 lie below a mixing line between the surface layer and the warm core of the Atlantic layer for all stations except NPEO'03-01. For all these profiles, for salinity greater than 34.6, O_2 concentrations increase into the warm core of the Atlantic layer.

5. Discussion

First-order spatial trends in our O_2 data are consistent with previous discussions of O_2 distributions in the Arctic Basin based on bottle data (Swift et al., 1997). Halocline O_2 "maxima" near the North Pole have not, however, previously been mentioned nor are they evident in climatologies. This cannot be taken as conclusive evidence that such features did not exist previously, though, since the bottle spacing can easily miss such features. Furthermore, extrema on these vertical scales are likely to disappear during the interpolation and averaging carried out to prepare climatological profiles.

To explain the structure we observed in the halocline, we propose the following. An *apparent* subsurface halocline O_2 maximum at the North Pole (NPEO'03-S1; Fig. 3) arises when Eurasian Basin waters, bearing O_2-depleted shelf waters, are advected in the sense of the Transpolar Drift, obliquely above the better ventilated boundary current along the Amundsen flank of the Lomonosov Ridge. Low oxygen concentrations are maintained immediately below the mixed layer of the Transpolar Drift via the isolation of these waters from the atmosphere. In addition, contributions of Pacific origin can feed waters with low oxygen concentrations into this layer. For example, fixed nitrogen–phosphate relationships at 5 and 62 m at NPEO'03-S1 indicate, respectively, 63% and 9% volume contributions from Pacific source waters (Falkner, 2003; Jones et al., 1998). This combination of limited ventilation and contribution of low O_2 Pacific shelf waters produces the low in O_2 at $S \approx 32.9$. With increasing depth, the influence of the Transpolar Drift is supplanted by that of the boundary current, and thus for $S > 33.2$, O_2 trends with the boundary current, i.e. initially increasing and then decreasing with increasing depth as seen in the NPEO'02-S3 oxygen profile. The influence of the relatively fresh portion of Transpolar Drift Stream is nicely illustrated in O_2-salinity space (Fig. 3) in the contrast between NPEO'02-S3 (where it is absent) and NPEO'03-S1. Intrusive structures in the halocline O_2 peak at NPEO'03-S1 result from interleaving of waters with differing O_2 properties.

Spatial trends of decreasing temperature, salinity, and O_2 in the core Atlantic layer from the North Pole to the Lincoln Sea show it to be progressively more distant from its origin in this direction. Meanwhile, along the same spatial track, Pacific inputs exert increasing influence in the upper layers. We propose that, analogously to our NPEO'03-S1 North Pole station, the vertical structure of water properties along this track is influenced by the Transpolar Drift Stream intermingling with underlying boundary current waters, in this case including waters from the Canada Basin. We propose that halocline O_2 maxima in our profiles and those reported by others (McLaughlin et al., 2004; Wilson and Wallace, 1990) primarily reflect input of O_2-depleted waters into relatively well-ventilated waters. As we discuss below, lateral injections of low-O_2 waters of both Pacific and Atlantic origin are a key component in generating such maxima. At this juncture, we cannot rule out contributions of the local O_2 "maxima" from O_2-enriched waters from the East Siberian or southern Beaufort seas, which may be produced in conjunction with ice production on the shelves (McLaughlin et al., 2004; Shimada et al., 2005). If such contributions occur, however, they result in maximal O_2

concentrations that correspond to saturations of $<70\%$, even close to their supposed shelf sources.

Summer 2002 CBL O_2 sensor data provide direct evidence for low O_2 inputs of Pacific origin in addition to the well-known wBSW. Our objective in referring to this data set is to show that waters of the appropriate source properties have been observed. The spatial extent of influence, volumes flows and persistence of such waters remain to be determined by future research. Note also that the low O_2 signals are accompanied by elevated nutrient signals to be presented in a future publication (Woodgate and Swift, unpublished data). Example profiles from the CBL cruise are shown in Fig. 4 (cf., Fig. 1b for locations). Station 21 is taken to be representative of waters entering the region immediately upstream of the Mendeleeyev Ridge. Stations 14 and 123 are situated in bathymetric indentations that cross the shelf, and they are representative of a series of closely spaced stations that show similar features. Stations 85 and 110 are likely downstream of outflows steered off the shelf through these indentations.

Near the head of the westernmost canyon (CBL-S14), unusually low O_2 ($<220\,\mathrm{mmol\,m^{-3}}$) occurred at $32.5<S<34.4$, with pronounced minima at both ends of this range. Low O_2 was associated with elevated temperatures across this salinity

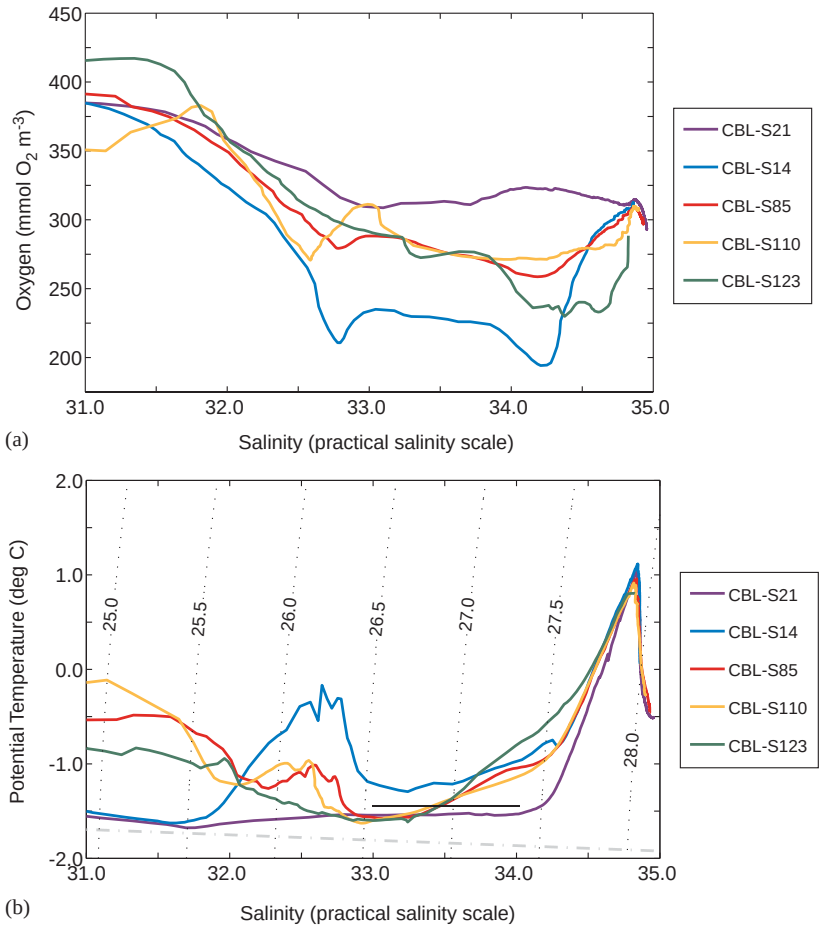

Fig. 4. Upper Panel: Dissolved oxygen vs. salinity at representative locations from the Chukchi Borderlands, August 2002 mission. For station locations see Fig. 1b. Lower Panel: Potential temperature vs. salinity for the same stations. Constant density lines (sigma–theta units) are superimposed.

range, with the shallower variant having the strongest expression in temperature. Quite low O_2 also occurs for $34 < S < 34.8$ at the eastern canyon (CBL-S123) and is again accompanied by elevated temperatures. Waters with characteristics such as these may be initially formed in winter when bottom waters are isolated from exchange with the atmosphere and are in contact with sediments where respiratory activities consume O_2 and regenerate dissolved nutrients. Subsequently, when the ice retreats around the Arctic perimeter, lower salinity waters warmed by summer insolation cap the denser water and prevent the underlying waters from free O_2 exchange with the atmosphere.

Downstream of the western canyon, CBL-S85 shows characteristics that are intermediate between those at the head of the canyon (CBL-S14) and those upstream of the Meneleeyev Ridge (CBL-S21). Likewise, properties at CBL-S110 can be derived through mixing of the Mendeleeyev Ridge waters (CBL-S21) and those from the canyons (CBL-S14 and 123). An important result of these interactions is that O_2 maxima of varying shapes are created at CBL-S85 and CBL-S110 as their constituent water types encounter one another. We note further that the complexities of these features would be difficult to capture by bottle sampling.

The AOS94 CTD oxygen sensor profiles (Fig. 5; locations on Fig. 1) further support our hypotheses on the origins of the halocline oxygen extrema found in our Alert-to-North Pole section. AOS94 station 9 was located on the Chukchi slope between the Mendeleyev Ridge and the Chukchi Borderlands above the $\approx$1700 m isobath, i.e., just offshore of the Chukchi shelf. Station 13 was located on the crest of the Mendeleyev Ridge at $\approx$1200 m. Stations 17 and 18 were located at $\approx$1700 and $\approx$2700 m on the eastern (Canadian) flank of the Mendeleyev Ridge, on the slope leading to the Mendeleyev Abyssal Plain, the western most arm of the deep Canada Basin. Station 26 lies in the central Makarov Basin at $\approx$3200 m. Station 33 lies at 89°N above the $\approx$3000 m isobath on the Eurasian flank of the Lomonosov Ridge. Finally, Station 36 was located in the northern Nansen Basin at $\approx$3500 m, immediately south of the Nansen-Gakkel Ridge.

The oxygen profiles at AOS94 stations 9 and 13 (Fig. 5) provide direct evidence of inputs of low O_2 water of Pacific origin. At station 9, the closest to the shelf, relatively low-oxygen waters are found over a broad range of salinities, from ca. 32.2 to 34. At station 13, farther north and at the Mendeleyev Ridge crest, the O_2-salinity distribution is nearly identical to that at station 9 for the upper-most waters, i.e. for salinities less than 33.4, but there is at that point a sharp jump to higher O_2 concentrations as salinity increases. Noting that intermediate waters along the Siberian boundary of the Makarov Basin were in 1994 nearly identical to those over the Eurasian flank of the Lomonosov Ridge (Swift et al., 1997), and comparing O_2-salinity relationships at stations 9 and 33 (Lomonosov Ridge flank) with that at station 13, it is apparent that well-ventilated Makarov basin boundary current waters, following the isobaths of the Mendeleyev Ridge north from the Siberian boundary, are at station 13 overlain by low salinity, low O_2 water from the Chukchi boundary. The AOS94 potential temperature–salinity relationship (Fig. 4) shows that much of the low-oxygen layer at station 9 is relatively warm, with the coldest low-O_2 waters at higher salinities. Low O_2 concentrations near salinities of 32.5 and 33.6 correspond to local temperature maxima with the less saline (shallower) variant having the strongest expression in temperature.

At station 13, the low-O_2 waters with salinities in the range 32.2–33.2 are relatively warm, but the higher-O_2 waters with salinities greater than 33.4 are cold, in fact almost identical in temperature and salinity to station 33 waters on the Eurasian slope of the Lomonosov Ridge. This leads us to conclude that, at least in this instance in 1994, an observed high oxygen layer in the halocline near the Chukchi Borderlands region is not water originating from the East Siberian Sea, but instead is water from a source in the Eurasian sector of the Arctic Ocean which has spread along the Makarov Basin's Siberian boundary. Silicate levels in the high oxygen, cold layer near $S = 33.7$ at AOS94 station 13 were low (ca. 7 mmol m^{-3}), entirely consistent with a Eurasian sector origin.

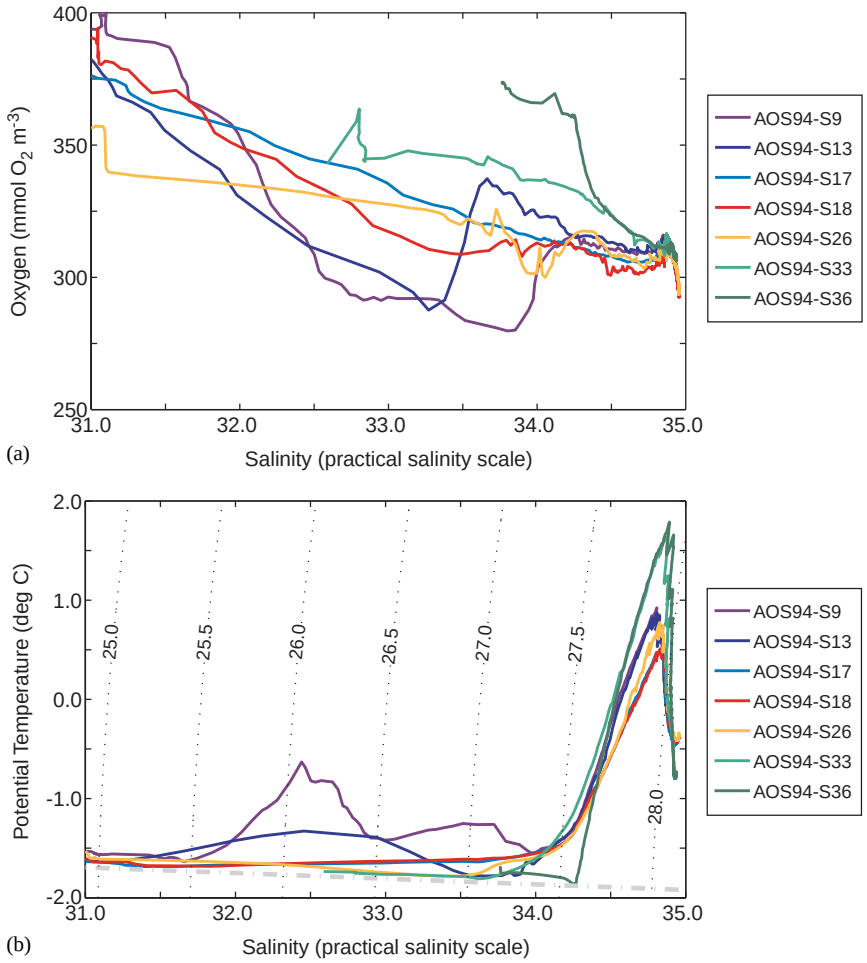

Fig. 5. Upper panel: Dissolved oxygen vs. salinity at locations from the AOS94 mission. For station locations see Fig. 1b. Lower panel: Potential temperature vs. salinity for the same stations. Constant density lines (sigma–theta units) are superimposed.

At AOS94 stations 17 and 18, on the remote Mendeleyev Ridge slope leading into the Canada Basin, and at station 26, in the central Makarov Basin, the O_2-salinity relationships through the halocline reflect competing influences of the low-O_2 shelf waters and high-O_2 Eurasian sector waters. (The station 26 O_2 profile minima near $S = 34$ (Fig. 5) was not seen in four bottle samples across the salinity range 33.77–34.19, and so we believe they are artifacts.)

The O_2-salinity relationship at AOS94 station 33 in the vicinity of the North Pole (Fig. 5) nicely illustrates the high-oxygen upstream boundary conditions for halocline waters in our Alert–North Pole transect. Oxygen concentrations there are high at every salinity above the Atlantic layer, providing precisely the water mass background required, as this water is carried to our study region, to generate O_2 maxima along our section due to interleaving with low-O_2 halocline waters such as though typical of the southern Canada Basin.

Given the origins, expressions of the low O_2 inputs can be expected to reflect temporal variability in the source properties and strength, as well as spatial variability in their distribution within the

Canada Basin. That such variability occurs has been confirmed for properties of wBSW in the southern Beaufort Sea (McLaughlin et al., 2002). Despite variability, certain characteristics of Pacific water sources seem to remain recognizable across a large portion of the Canada Basin over the last several decades. As discussed in the background section, a local temperature maximum in the salinity range 32–33 evident at CBL-S14, 85 and 110 and AOS94 station 9 and 13, has previously been identified as sBSW and mapped across much of the northern Beaufort Gyre (Coachman and Barnes, 1961; Steele et al., 2004). If it was also O_2-depleted, such sBSW could be influencing our NPEO and SWYD profiles, with the strongest expression occurring at SYWD'03-S5 (Fig. 3). At this station, the local temperature maximum near 80 m is contiguous with the underlying the local temperature minimum of wBSW near 110 m, and the two components intersect to generate the lowest O_2 levels over this salinity range for the North Pole to Ellesmere section.

What appear to be prominent local O_2 maxima over $33.2 < S < 33.8$ in NPEO'03-S6 and SWYD'03-S8 have coincident expressions in temperature minima. These minimum temperatures approach values observed at NPEO'03-S5 that are associated with relatively high O_2 (Fig. 3). Thus, such O_2 maxima over the slope may reflect either advection of O_2 extrema with the large-scale circulation, or lateral mixing with adjacent offshore waters. Likewise, the broader apparent O_2 maxima at SWYD'03-S4 and S5 over a similar salinity range are coincident with equally broad minima in temperature that again approach those of NPEO'03-S5 over the same salinity range. The O_2 concentrations in these features are well below saturation. This, together with smoothness of the properties over a broad depth range, suggest to us mixing at the confluence of major currents rather than O_2 injection events. Such O_2 structures diminish southward over the shelf break transect (Fig. 3).

At higher salinity, additional sources of low O_2 water come into play. The CBL data shows O_2 depletions can occur centered on about 34.1 and 34.6 (Fig. 4), and these are associated with temperatures well above freezing. It is not clear from this one-time sampling whether these O_2 minima represent regionally significant inputs or more restricted local products. Low O_2 at $S \approx 34.7$ would contribute to reinforcing the minimum at that depth inherited upstream in the Eurasian Basin and it would also explain the pronounced O_2 depletion in this layer, contrasting with the underlying O_2 maximum below the Atlantic layer temperature maximum. Thus the shapes of our profiles in this higher salinity range can be understood as resulting from the varying influence of such source waters.

We note also that our NPEO'03 results are not consonant with a simple cyclonic boundary current scheme (Fig. 1b) for circulation of Atlantic waters in the eastern Makarov Basin. Such schemes imply that NPEO'03-S4 should be more evolved (lower T, S and O_2) than NPEO'03-S5, while the opposite appears to be true (Figs. 3 and 4). An earlier trace gas study also suggested that a cyclonic circulation scheme did not apply to this part of the Makarov Basin, since the least ventilated waters were found over the Alpha Ridge (Smethie et al., 2000; Smith et al., 1999). Likely the complex bathymetry in the region contributes to an equally complex circulation (Fig. 1b).

6. Conclusions

Here we have presented evidence that injection of low O_2 Pacific and Atlantic source waters into the large-scale circulation can generate apparent O_2 maxima in layers between. Apparent nutrient minima can be expected to accompany these apparent O_2 maxima, as was noted in some of the SHEBA drift data (McLaughlin et al., 2004). While it has been known for some time that wBSW is O_2-depleted and nutrient enriched, we show for the first time that sBSW, which has been mapped throughout much of the Canada Basin, is likewise characterized. Additional Pacific inputs can serve to reinforce the O_2 minimum centered at $S \approx 34.7$ that occurs throughout the majority of the Makarov and Canada basins. While it remains to be proven how persistent and pervasive these sources are, their influence appears to be exerted

far downstream. Previous reports of O_2 maxima over the Alpha Ridge (Wilson and Wallace, 1990) can now be understood as arising from the combined effects of the $S \approx 34.7$ O_2 minimum that originates in the Eurasian sector and O_2-deficient Pacific sources, e.g., the 33.1 wBSW. Since profile-to-profile differences probably reflect the different trajectories of these source waters, well-calibrated sensor-based O_2-mapping should provide an effective means for clarifying those trajectories in the future. Finally, if injection of O_2-enriched waters into the halocline does occur, as has been proposed by others, this must entail entrainment of significant amounts of O_2-depleted water, since concentrations in the apparent maxima remain well below saturation at all of the locations for which they have been reported to date.

Acknowledgements

We wish to acknowledge essential contributions to this manuscript by C. Meredith and S. Gard of OSU. We thank R. Anderson of APL-UW for collaborating on the processing of the CTD-O_2 data. Coordination and success of the logistics support for NPEO and SWYD rests on the apt shoulders of A. Heiberg. We are appreciative of helpful comments by three thoughtful reviewers. Funding for this program has been provided through Arctic System Sciences of the Office of Polar Programs of NSF (#9910335 to KKF; #9910305 to KA; #0117480 to RAW; #0230427 to MS; # to JM).

References

Aagaard, K., Coachman, L.K., Carmack, E.C., 1981. On the halocline of the Arctic Ocean. Deep-Sea Research 28, 529–545.

Broecker, W.S., 1974. "NO", A conservative water-mass tracer. Earth and Planetary Science Letters 23, 100–107.

Carmack, E.C., Aagaard, K., Swift, J.H., Macdonald, R.W., McLaughlin, F.A., Jones, E.P., Perkin, R.G., Smith, J.N., Ellis, K.M., Kilius, L.R., 1997. Changes in the temperature and tracer distributions within the Arctic Ocean: results from the 1994 Arctic Ocean Section. Deep-Sea Research II 44 (8), 1487–1502.

Carmack, E.C., Aagaard, K., Swift, J.H., Perkin, R.G., McLaughlin, F.A., Macdonald, R.W., Jones, E.P., 1998. Thermohaline transitions. In: Jörg Imberger (Ed.), Physical Processes in Lakes and Oceans. American Geophysical Union, pp. 179–186.

Coachman, L.K., Barnes, C.A., 1961. The contribution of Bering Sea water to the Arctic Ocean. Arctic 14, 147–161.

Coachman, L.K., Aagaard, K., Tripp, R.B., 1975. Bering Strait: The Regional Physical Oceanography. UW Press, Seattle 172pp.

Codispoti, L.A., Richards, F.A., 1971. Oxygen supersaturations in the Chukchi and East Siberian Seas. Deep-Sea Research 18, 341–351.

Codispoti, L.A., Friederich, G.E., Sakamato, C.M., Gordon, L.I., 1991. Nutrient cycling and primary production in the marine systems of the Arctic and Antarctic. Journal of Marine Systems 2, 359–384.

Cooper, L.W., Whitledge, T.E., Grebmeier, J.M., Weingartner, T., 1997. The nutrient, salinity, and stable oxygen isotope composition of Bering and Chukchi Seas waters in and near Bering Strait. Journal of Geophysical Research 102 (C6), 12563–12573.

Dickson, A.G., 1994. Determination of Dissolved Oxygen in Sea Water by Winkler Titration. WOCE Hydrographic Program, Woods Hole, MA, pp. 11.

Falkner, K.K., 2000–2001. Seawater chemistry from the North Pole Environmental Observatory. National Snow and Ice Data Center., Boulder, CO.

Falkner, K.K., 2002. Seawater Chemistry from the North Pole Environmental Observatory. National Snow and Ice Data Center., Boulder, CO.

Falkner, K.K., 2003. Seawater Chemistry from the North Pole Environmental Observatory. National Snow and Ice Data Center., Boulder, CO.

Guay, C.K., Falkner, K.K., 1997. Barium as a tracer of Arctic halocline and river waters. Deep-Sea Research II 44 (8), 1543–1569.

Jones, E.P., Anderson, L.G., 1986. On the origin of the chemical properties of the Arctic Ocean halocline. Journal of Geophysical Research 91, 10759–10767.

Jones, E.P., Anderson, L.G., Wallace, D.W.R., 1991. Tracers of near-surface, halocline and deep waters in the Arctic Ocean: Implications for circulation. Journal of Marine Systems 2, 241–255.

Jones, E.P., Anderson, L.G., Swift, J.H., 1998. Distribution of Atlantic and Pacific waters in the upper Arctic Ocean: Implications for circulation. Geophysical Research Letters 25 (6), 765–768.

Joyce, T., Corry, C., 1994. WOCE Operations Manual, Volume 3: The Observational Programme, Section 3.1: WOCE Hydrographic Programme, Part 3.1.3: WHP Operations and Methods, Revision 1. Woods Hole, Mass.

Kinney, P., Arhelger, M.E., Burrell, D.C., 1970. Chemical characteristics of water masses in the Amerasian Basin of the Arctic Ocean. Journal of Geophysical Research 75, 4097–4104.

McLaughlin, F.A., Carmack, E.C., Macdonald, R.W., Bishop, J.K.B., 1996. Physical and geochemical properties across the Atlantic/Pacific water mass front in the southern Canadian Basin. Journal of Geophysical Research 101 (C1), 1183–1197.

McLaughlin, F., Carmack, E., Macdonald, R., Weaver, A.J., Smith, J., 2002. The Canada Basin, 1989–1995: Upstream events and far-field effects of the Barents Sea. Journal of Geophysical Research 107 (C7).

McLaughlin, F.A., Carmack, E.C., Macdonald, R.W., Melling, H., Swift, J.H., Wheeler, P.A., Sherr, B.F., Sherr, E.B., 2004. The joint roles of Pacific and Atlantic-origin waters in the Canada Basin, 1997–1998. Deep Sea Research I 51, 107–128.

Melling, H., Moore, R.M., 1995. Modification of halocline source waters during freezing on the Beaufort Sea shelf: evidence from oxygen isotopes and dissolved nutrients. Continental Shelf Research 15 (1), 89–113.

Moore, R.M., Smith, J.N., 1986. Disequilibria between ^{226}Ra, ^{210}Pb and ^{210}Po in the Arctic Ocean and the implications for chemical modification of the Pacific water inflow. Earth and Planetary Science Letters 77, 285–292.

Morison, J.H., Aagaard, K., Falkner, K.K., Hatakeyama, K., Moritz, R., Overland, J.E., Perovich, D., Shimada, K., Steele, M., Takizawa, T., Woodgate, R., 2002. The North Pole Environmental Observatory. EOS, Transactions of the American Geophysical Society 83 (33), 357–361.

Owens, W.B., Millard, R.C.J., 1985. A new algorithm for CTD oxygen calibration. Journal of Physical Oceanography 15, 621–631.

Quadfasel, D., Sy, A., Rudels, B., 1993. A ship of opportunity section to the North Pole: upper ocean temperature observations. Deep-Sea Research I 40 (4), 777–789.

Rudels, B., Anderson, L.G., Jones, E.P., 1996. Formation and evolution of the surface mixed layer and halocline of the Arctic Ocean. Journal of Geophysical Research 101 (C4), 8807–8821.

Salmon, D.K., McRoy, C.P., 1994. Nutrient-based tracers in the Western Arctic: A new lower halocline water defined. In: Johannessen, O.M., Muench, R.D., Overland, J.E. (Eds.), The Polar Oceans and Their Role in Shaping the Global Environment. AGU, Washington, DC, pp. 47–62.

Schauer, U., Rudels, B., Jones, E.P., Anderson, L.G., Muench, R.D., Björk, G., Swift, J.H., Ivanov, V., Larsson, A.-M., 2002. Confluence and redistribution of Atlantic water in the Nansen, Amundsen and Makarov basins. Annales Geophysicae 20, 257–273.

Sherr, B.F., Sherr, E.B., 2003. Community respiration/production and bacterial activity in the upper water column of the central Arctic Ocean. Deep-Sea Research I 50, 529–542.

Shimada, K., Itoh, M., Nishino, S., McLaughlin, F., Carmack, E., Proshutinsky, A., 2005. Halocline structure in the Canada Basin of the Arctic Ocean. Geophysical Research Letters 32, L03605.

Smethie, W.M.J., Schlosser, P., Bonisch, G., Hopkins, T.S., 2000. Renewal and circulation of intermediate waters in the Canadian Basin on the SCICEX 96 cruise. Journal of Geophysical Research 105 (C1), 1105–1121.

Smith, J.N., Ellis, K.M., Boyd, T., 1999. Circulation features in the Central Arctic Ocean revealed by nuclear fuel reprocessing tracers from SCICEX 95 and 96. Journal of Geophysical Research 104, 29633–29677.

Steele, M., Morison, J., Ermold, W., Rigor, I., Ortmeyer, M., Shimada, K., 2004. Circulation of summer Pacific halocline water in the Arctic Ocean. Journal of Geophysical Research 109 (C2), C02027.

Swift, J.H., Jones, E.P., Aagaard, K., Carmack, E.C., Hingston, M., Macdonald, R.W., McLaughlin, F.A., Perkin, R.G., 1997. Waters of the Makarov and Canada basins. Deep-Sea Research II 44 (8), 1503–1529.

Wallace, D.W.R., Moore, R.M., Jones, E.P., 1987. Ventilation of the Arctic Ocean cold halocline; Rates of diapycnal and isopycnal transport, oxygen utilization and primary production inferred using chlorofluoromethane distributions. Deep-Sea Research 34, 1957–1979.

Weingartner, T.J., Cavalieri, D.J., Aagaard, K., Sasaki, Y., 1998. Circulation, dense water formation, and outflow on the northeast Chukchi shelf. Journal of Physical Research 103 (C4), 7647–7661.

Wilson, C., Wallace, D.W.R., 1990. Using the nutrient ratio NO/PO as a tracer of continental shelf waters in the central Arctic Ocean. Journal of Geophysical Research 95 (C12), 22193–22208.